BMB
*Reports*

**BMB Rep. 2015; 48(6): 342-347**
www.bmbreports.org

# Insulin activates EGFR by stimulating its interaction with IGF-1R in low-EGFR-expressing TNBC cells

*Miyoung Shin*[1,2], *Eun Gyeong Yang*[2], *Hyun Kyu Song*[1,*] *& Hyesung Jeon*[2,3,*]

[1]Division of Life Sciences, Korea University, Seoul 136-701, [2]Center for Theragnosis, Biomedical Research Institute, Korea Institute of Science and Technology, Seoul 136-791, Korea, [3]Department of Cancer Biology, Dana-Farber Cancer Institute, Boston, MA 02215, USA

**The expression of epidermal growth factor receptor (EGFR) is an important diagnostic marker for triple-negative breast cancer (TNBC) cells, which lack three hormonal receptors: estrogen and progesterone receptors as well as epidermal growth factor receptor 2. EGFR transactivation can cause drug resistance in many cancers including TNBC, but the mechanism underlying this phenomenon is poorly defined. Here, we demonstrate that insulin treatment induces EGFR activation by stimulating the interaction of EGFR with insulin-like growth factor receptor 1 (IGF-1R) in the MDA-MB-436 TNBC cell line. These cells express low levels of EGFR, while exhibiting high levels of IGF-1R expression and phosphorylation. Low-EGFR-expressing MDA-MB-436 cells show high sensitivity to insulin-stimulated cell growth. Therefore, unexpectedly, insulin stimulation induced EGFR transactivation by regulating its interaction with IGF-1R in low-EGFR-expressing TNBC cells. [BMB Reports 2015; 48(6): 342-347]**

## INTRODUCTION

Triple-negative breast cancers (TNBCs) are estrogen receptor-negative ($ER^-$), progesterone receptor-negative ($PR^-$), and human epidermal growth factor receptor 2-negative ($HER2^-$). This class of cancers is associated with poorer prognosis and increased visceral metastasis compared to hormone receptor-positive breast cancers (1). Tissue microarray studies on a basal-like breast cancer subtype that overlaps with 60-90% of TNBC indicate that epithermal growth factor receptor (EGFR/HER1/ErbB-1) expression is a biomarker that can be used to define a molecular phenotype (2). EGFR overexpression is common in TNBCs and abnormal activation of EGFR signaling often causes drug resistance to anti-estrogen therapy (3, 4). However, clinical trials have shown that EGFR targeting using monoclonal antibodies or tyrosine kinase inhibitors has limited effectiveness in breast cancer patients (5). One possible explanation for these limitations is that EGFR transactivation has been shown to increase IGF-1R signaling, increasing the resistance of cancers to anti-EGFR treatment (6). Moreover, enhanced IGF-1R pathway activation plays an important role in the maintenance of cellular functions in a variety of cancer cell types that are resistant to anti-EGFR therapies (7-9). Because IGF-1R signaling is upregulated in cancer cells treated with anti-EGFR therapies, co-targeting of IGF-1R and EGFR could be a useful strategy for improving the therapeutic efficacy of anti-EGFR agents in clinical studies (10). Activated EGFR triggers two representative signaling pathways, RAS/MEK/ERK and PI3K/AKT. Both pathways are involved in critical cellular processes such as apoptosis inhibition, cell migration, cell growth, and angiogenesis, but the latter pathway has also been implicated in the critical mechanism of therapeutic resistance and breast cancer survival (11). According to a recent report in which TNBC subtypes were classified (12), the MDA-MB-468 cell line is considered to be a basal-like subtype, while the MDA-MB-436 cell line is a mesenchymal-like subtype with a much lower response to taxane-based therapies. In contrast to MDA-MB-468 cells that express a high level of EGFR (13), MDA-MB-436 cells express very low levels of EGFR and high levels of activated IGF-1R. Thus, we investigated the interaction between EGFR and IGF-1R in TNBC cell lines in the presence of insulin stimulation. Our data clearly show that the interaction between EGFR and IGF-1R increases in response to insulin treatment, subsequently increasing EGFR internalization in MDA-MB-436 cells, but not in MDA-MB-468 TNBC cells. These data suggest that each TNBC type should be characterized with respect to EGFR and IGF-1R pathways. Because TNBCs are diverse and complicated, proper subtyping in this manner could be valuable for the treatment of breast cancer patients.

*Corresponding authors. Hyun Kyu Song, Tel: +82-2-3290-3457; Fax: +82-2-3290-3628; E-mail: hksong@korea.ac.kr, Hyesung Jeon, Tel: +1-617-632-4398, Fax: +1-617-632-4393, E-mail: hjeon@red.dfci.harvard.edu

http://dx.doi.org/10.5483/BMBRep.2015.48.6.157

**Received 31 July 2014, Revised 22 August 2014, Accepted 21 October 2014**

**Keywords:** EGFR activation, IGF-1R interaction, Insulin, MDA-MB-436, Triple-negative breast cancer cells

ISSN: 1976-670X (electronic edition)

## RESULTS AND DISCUSSION

### Insulin enhances cell growth in a low-EGFR-expressing TNBC cell line

The role of IGF-1R in cancer development has been studied using animal models including those of early prostate and mammary cancer, as well as in lung cancer cell lines (14-16). In rodents, both exogenous and endogenous insulin induce the growth of transplanted cancer cells, but it is not clear whether tumor growth is caused by a direct effect on insulin receptors (IR) or on IGF-1R signaling (17). To investigate the responsiveness of different TNBC cell lines to insulin treatment, we examined the endogenous expression levels of growth factor receptors in three TNBC cell lines: MDA-MB-436, MDA-MB-231, and MDA-MB-468. Immunoblot analyses showed that each TNBC cell line had differential expression levels of the two growth factor receptors, IGF-1R and EGFR (Fig. 1A). IGF-1R expression and phosphorylation levels were particularly high in the low-EGFR-expressing MDA-MB-436 cells. In contrast, MDA-MB-468 cells, which are known to have a high level of EGFR, had modest levels of IGF-1R expression and phosphorylation that were unaffected by insulin. MDA-MB-436 cells incubated in complete medium containing 5 μg/mL of insulin for 3 days had an increased growth rate that was greater than that observed for the other TNBC cell lines (Fig. 1B). According to previous studies, insulin levels correlate with tumor growth and IR/IGF-1R signaling (18, 19). IR/IGF-1R tyrosine kinase inhibitor treatments inhibit growth in mammary tumors (20, 21). However, resistance to IGF-1R signaling inhibitors has been reported, suggesting that this receptor might induce downstream PI3K/mTOR signaling through the activation of EGFR signaling (22, 23). Because the growth rate of MDA-MB-436 cells was increased by insulin, we examined cell proliferation in these cells by performing an MTS assay. As shown in Figure 1C, the absorbance of MDA-MB-436 cells at 490 nm increased by approximately 10%. MDA-MB-231 cells, on the other hand, were not significantly affected and MDA-MB-468 cells showed a slight reduction in absorbance at 490 nm. These results reaffirmed that the viability of MDA-MB-436 cells was more sensitive to insulin than other cell lines. To further support the observation that insulin stimulation affected cell survival, we examined cell viability after a 6-h treatment with staurosporine, an inducer of apoptotic cell death (Fig. 1D). All cell types were affected by staurosporine, reducing their viability to ~75%. However, insulin-treated MDA-MB-436 cells maintained slightly higher viability after induction of apoptosis.

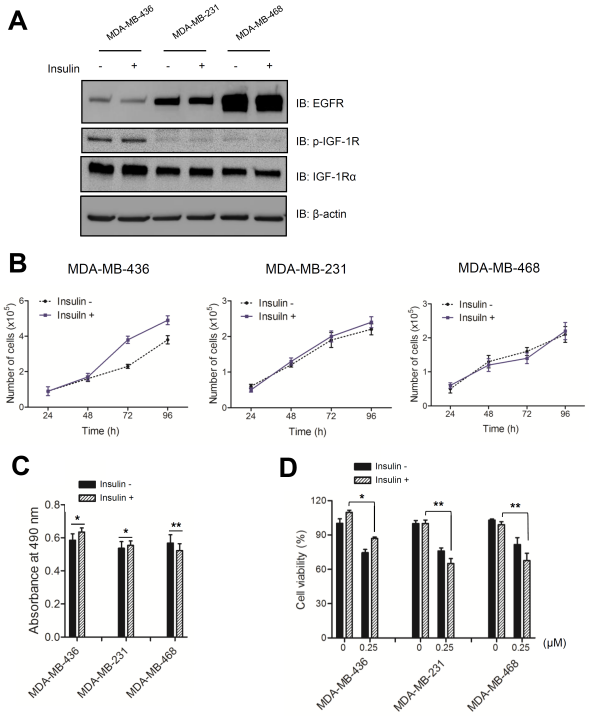


**Fig. 1.** Insulin stimulates cell growth in an IGF-1R-activated TNBC cell line. (A) Cells were cultured in the presence (+) or absence (−) of 5 μg/ml insulin. Immunoblot analysis of lysates was performed using anti-EGFR, anti-IGF-1R, and anti-p-IGF-1R antibodies. (B) Growth curves for each TNBC cell line treated with 5 μg/ml insulin were constructed using GraphPad software. The error bars were calculated based on three independent experiments. Values plotted are the means ± standard deviation (SD; n = 3). (C) Cells were cultured in the presence of 5 μg/ml insulin for 3 d and then treated with MTS solution for 1 h. The absorbance was measured at 490 nm. (D) TNBC cell lines were cultured in the presence of 5 μg/ml insulin for 3 d, treated with staurosporine (0 or 0.25 μM) for 6 h and then an MTS assay was performed. Statistical values for the MTS assay are expressed as the means ± SD (n = 3; Student's t-test, *P < 0.05, **P < 0.001).

### Insulin induces interactions between EGFR and IGF-1R in MDA-MB-436 cells

Previous studies have reported a connection between EGF and insulin signaling in human breast cancer cells, which occurs through the interaction of EGFR and IGF-1R (24, 25). IGF-1R knockdown experiments in MDA-MB-436 cells were performed using a validated specific siRNA (Fig. 2B). We used confocal imaging to confirm that IGF-1R expression correlated with EGFR internalization in response to insulin stimulation (Fig. 2C). To further examine the relationship between these two receptors in response to insulin treatment, we performed a proximal ligation assay (PLA), which can show interactions be-

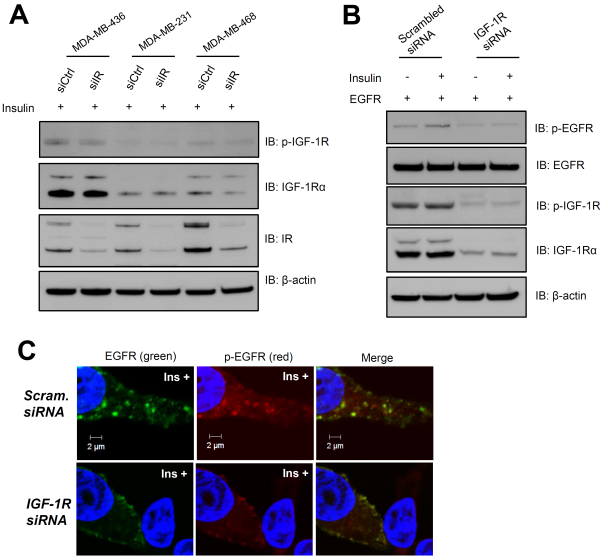


**Fig. 2.** IGF-1R is required for transactivation of insulin-stimulated EGFR. Cells were stimulated with 10 μg/ml insulin for 1 h after siRNA transfection was performed for 48 h. (A) Immunoblot analysis was performed for three TNBC cell lines (MDA-MB-436, -231, and -468) transfected with IR siRNA or scrambled siRNA control by using anti-IGF-1R, anti-p-IGF-1R (Y1280), and anti-IR antibodies. (B) siRNA-mediated suppression of IGF-1R expression in MDA-MB-436 cells expressing exogenous EGFR. Immunoblot analysis was performed using anti-p-EGFR, anti-EGFR, and anti-p-IGF-1R (Y1280), and anti-IGF-1R antibodies on cells transfected with IGF-1R siRNA or scrambled siRNA control. (C) EGFR phosphorylation and internalization upon insulin stimulation were examined in cells transfected with IGF-1R siRNA or scrambled siRNA control. Scale bar, 2 μm. Ins, insulin.

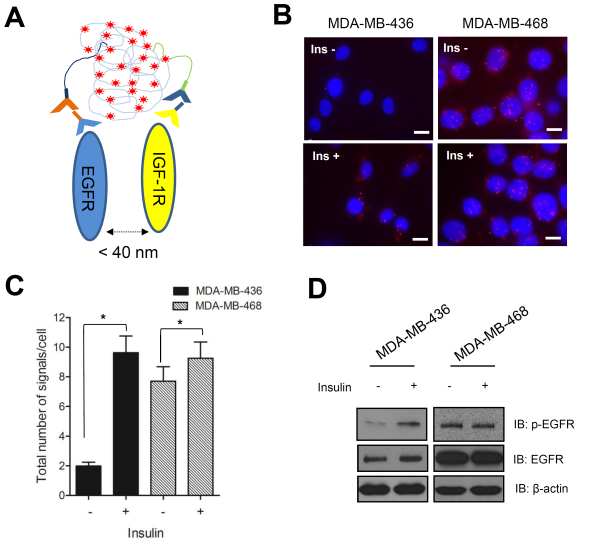


**Fig. 3.** Insulin induces interaction between EGFR and IGF-1R. Cells were stimulated with 10 μg/ml insulin for 1 h after treatment in serum-free media containing 30 μg/mL cycloheximide for 8 h. (A) Schematic figure showing the principle of proximal ligation assay. (B) Proximity ligation assay was performed according to the manufacturer's instructions and cell images were obtained using fluorescence microscopy (Applied Precision Delta Vision, 60× oil objective with a 1.35 numerical aperture). Red dots indicate signals resulting from the interaction between EGFR and IGF-1R. Nuclei were counterstained with 4',6-diamidino-2-phenylindole (DAPI, blue). Scale bar, 10 μm. Ins, insulin. (C) Cell images were analyzed using the Duolink® ImageTool software and statistical analyses were performed using GraphPad software. Error bars in the graph represent SD (n = 3; Student's t-test, *P < 0.05). (D) Immunoblot analysis was performed using anti-EGFR and anti-p-EGFR on MDA-MB-436 and -468 cell lines, respectively.

tween closely located molecules, by using specific primary antibodies against EGFR and IGF-1R (Fig. 3A). PLA signals, shown as red fluorescence in Fig. 3B, increased to a greater extent in MDA-MB-436 cells than in MDA-MB-468 cells in response to insulin treatment. The total number of signals per cell represents the interactions between EGFR and IGF-1R (Fig. 3C). The signals in MDA-MB-436 cells increased 5-fold in response to insulin treatment. On the other hand, no significant increase in the PLA signals were observed in MDA-MB-468 cells treated with insulin. Because MDA-MB-468 cells expressed a high level of EGFR and a relatively low level of IGF-1R, the presence of insulin may not increase the cross-talk between the two receptors. To verify the activation of EGFR in insulin-treated MDA-MB-436 cells, we performed an immunoblot to detect phosphorylated EGFR. As we expected, EGFR phosphorylation increased dramatically, but only in MDA-MB-436 cells (Fig. 3D). Therefore, we conclude that insulin stimulates EGFR transactivation through its interaction with IGF-1R in these cells.

## EGFR phosphorylation and internalization are enhanced by insulin in MDA-MB-436 cells

Using cellular imaging, we examined the internalization of EGFR in MDA-MB-436 cells in response to insulin stimulation. Images obtained using Alexa Fluor® 488-conjugated anti-EGFR antibody showed that endogenous EGFR was localized to the plasma membrane in the absence of insulin stimulation, but became localized primarily inside membrane-bound or cytoplasmic compartments in the presence of insulin (Fig. 4A). In contrast, no significant differences were observed in MDA-MB-468 cells in the presence or absence of insulin, as we expected. Although the result was not dramatic, more EGFR was distributed in the cytosolic fraction of MDA-MB-436 cells upon insulin stimulation (Fig. 4B). These data were consistent with the discovery that MDA-MB-436 cells containing lower levels of endogenous EGFR were more sensitive to insulin stimulation. We examined the phosphorylation status of EGFR in MDA-MB-436 and -468 cells using immunoprecipitation to confirm the activation of signaling in response to insulin treatment. We overexpressed EGFR in MDA-MB-436 cells to a

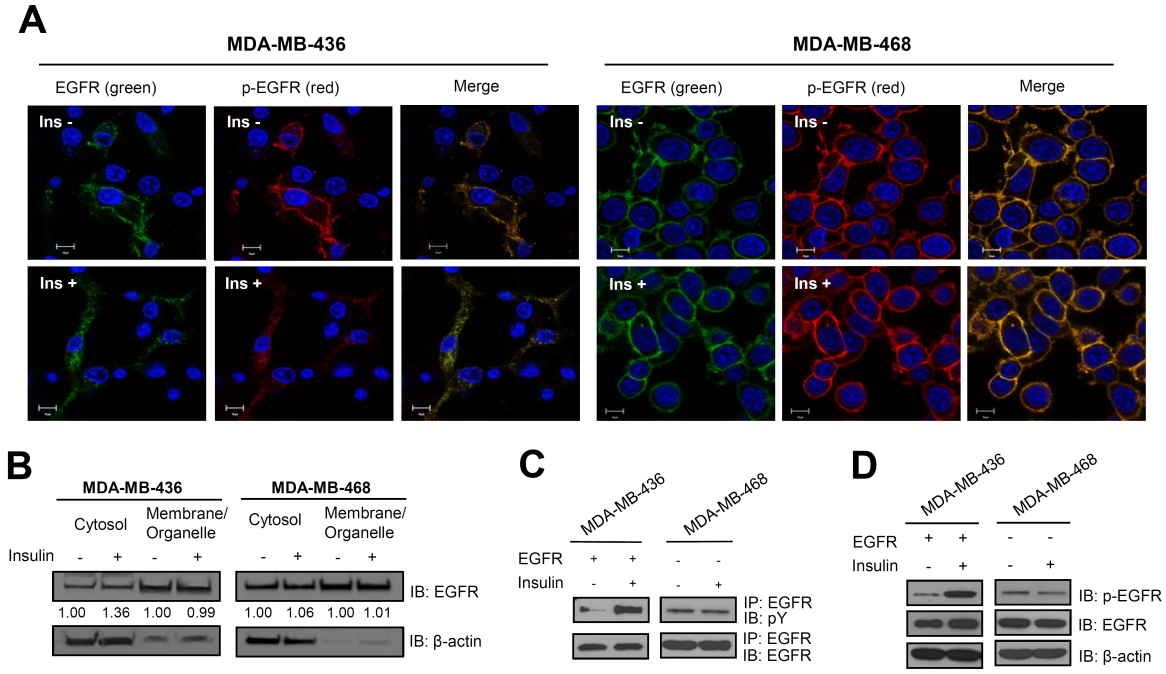


**Fig. 4.** Insulin increases EGFR phosphorylation and internalization. Cells were stimulated with 10 μg/mL insulin for 1 h after treatment in serum-free media containing 30 μg/ml cycloheximide for 8 h. (A) An immunofluorescence assay was performed using anti-EGFR antibody conjugated to Alexa Fluor® 488 and anti-p-EGFR, which was detected using Alexa Fluor® Rhodamine-conjugated anti-mouse IgG. Nuclei were counterstained with DAPI in transiently EGFR-transfected MDA-MB-436 cells and in MDA-MB-468 cells. Cell images were obtained using confocal microscopy (Carl Zeiss LSM700, 63× oil objective with a 1.4 numerical aperture). Scale bar, 10 μm. Ins, insulin. (B) Immunoblot analysis of subcellular compartments was performed using anti-EGFR after cell fractionation in MDA-MB-436 and -468 cell lines. The relative differences in band densities were analyzed using Image J software. (C) Immunoprecipitation was performed using anti-EGFR antibodies and blots were probed using anti-EGFR and anti-pY antibodies. (D) Immunoblot analysis was performed using anti-EGFR and anti-p-EGFR (Y1045) antibodies on transiently EGFR-transfected MDA-MB-436 cells and in MDA-MB-468 cells.

level comparable to that in MDA-MB-468 cells. Using immunoprecipitation, we showed that the addition of insulin increased the total phosphorylation of EGFR in EGFR-transfected MDA-MB-436 cells (Fig. 4C). The increased phosphorylation of EGFR at residue Y1045, the initial activation site involved in EGFR internalization, was confirmed by performing immunoblot analysis (Fig. 4D) on untransfected MDA-MB-436 cells (Fig. 3D). Therefore, EGFR and IGF-1R interact, and EGFR phosphorylation and internalization are stimulated by insulin treatment in a cell-type specific manner. These data are consistent with the confocal imaging results (Fig. 2C) obtained using IGF-1R siRNA-transfected MDA-MB-436 cells. Although the underlying mechanism by which insulin stimulation induces EGFR phosphorylation and internalization without affecting IGF-1R phosphorylation remains to be elucidated, activated p-EGFR clearly interacts with IGR-1R at the molecular level in the low-EGFR-expressing TNBC cell line MDA-MB-436. In contrast, EGFR in the high-EGFR-expressing cell line MDA-MB-468 was not affected by insulin (Fig. 4A). The signal transduced by EGFR and IGF-1R cross-talk might induce resistance toward specific EGFR-targeting drugs. Therefore, this pathway warrants further investigation for the purpose of improving treatments for patients with drug-resistant TNBC.

## MATERIALS AND METHODS

### Cell lines and culture conditions

MDA-MB-436 and MDA-MB-468 cell lines were purchased from the American Type Culture Collection (ATCC®) and cultured at 37°C and 5% $CO_2$ in RPMI 1640 medium supplemented with 10% (v/v) fetal bovine serum containing 100 U/ml penicillin and 100 μg/ml streptomycin, in the presence or absence of 5 μg/mL insulin (Sigma). The MDA-MB-231 cell line was obtained from the Korea Cell Line Bank (KCLB®) and maintained under the same conditions.

### Cell transfection and proliferation assay

Approximately 1.0 × $10^5$ cells were plated and the plasmids were transfected using the FuGENE® HD Transfection Reagent (Promega) according to the manufacturer's protocol. Cell proliferation was measured at 490 nm absorbance after incubation for 1 h in Cell Titer 96® Aqueous One Solution (Pro-

mega), containing 3-(4,5-dimethylthiazol-2-yl)-5-(3-carboxymethoxyphenyl)-2-(4-sulfophenyl)-2H-tetrazolium, inner salt (MTS) solution.

### siRNA transfection

siRNA oligonucleotide transfection was performed using Lipofectamine® RNAiMAX reagent (Invitrogen) according to the manufacturer's instructions. Cells were seeded and grown to 50-60% confluency on 100-mm culture dishes, incubated for 24 h, and then transfected with 10 nM of siRNAs against IGF-1R (product no. 100424, Bioneer), IR (product no. 100418, Bioneer), or a scrambled control siRNA (control siRNA-A, Santa Cruz) for 48 h.

### Immunoblot analysis and antibodies

Cells were lysed at 4°C in lysis buffer (50 mM Tris-HCl, pH 8.0, 0.15 M NaCl, 1% Nonidet P-40, and protease inhibitor cocktail). Following a 40-min incubation on ice, protein extracts were centrifuged at 15,000 × g for 10 min at 4°C. The amount of protein in the clarified supernatants was measured using Bradford Reagent (Sigma). Lysates were diluted with sodium dodecyl sulfate (SDS) sample buffer (0.4 M SDS, 0.4 M Tris-HCl, 40 mM EDTA, 50% glycerol, and bromophenol blue). The lysates were separated using SDS polyacrylamide gel electrophoresis and transferred to a nitrocellulose membrane using an iBLOT system (Invitrogen). Membranes were blocked in Tris-buffered saline containing 0.1% Tween 20 and 5% nonfat dry milk, and then incubated with the following specific primary antibodies: anti-EGFR, anti-IGF-1R, anti-p-EGFR (Tyr1045), anti-p-IGF-1R (Tyr1280), anti-pY (Santa Cruz). Horseradish peroxidase-conjugated anti-rabbit or anti-mouse IgG was used as the secondary antibody (Dako). Immunoreactive protein was visualized by chemiluminescence using the SuperSignal® West Pico Luminol/Enhancer Solution (Thermo Scientific). Equal protein loading was evaluated using an anti-$\beta$-actin antibody (Sigma).

### Immunoprecipitation

After 48 h of transfection, the cells were stimulated with insulin and cell lysates were prepared using lysis buffer. The clarified lysate supernatants were isolated using centrifugation and incubated with anti-EGFR antibodies overnight at 4°C. Next, pre-washed protein G Sepharose™ 4 Fast Flow (GE Healthcare) was mixed with the lysates using a laboratory tube rotator for 2 h at 4°C. Beads were washed several times and immunoblotting was then performed.

### Immunofluorescence assay

Cells were seeded at a density of ~1.0 × $10^5$ cells in coverglass- bottomed dishes (SPL Life Sciences) and incubated for 24 h (26). Cells were fixed with ice-cold 100% methanol for 20 min at −20°C and washed twice with PBS. Fixed cells were incubated for 1 h at room temperature (RT) in 10% bovine serum diluted in PBS and then with the primary antibodies for 3 h at RT. Alexa Fluor Dye®-conjugated anti-rabbit or anti-mouse IgG (Molecular Probes) were used as the secondary antibodies and were incubated with the cells for 1 h. After the cells were washed, the nuclei were counterstained using 4',6-diamidino-2-phenylindole (DAPI; Invitrogen). Images were obtained using a Delta Vision fluorescence microscope (Applied Precision) and LSM700 confocal microscope (Carl Zeiss).

### *In situ* proximity ligation assay

A Duolink® (Olink Biosciences) *in situ* proximity ligation assay was performed following the manufacturer's instructions. Briefly, cells were fixed with ice-cold 100% methanol for 20 min at −20°C and washed twice with PBS. Fixed cells were incubated in 10% bovine serum in PBS for 1 h at RT and then with the two primary antibodies anti-EGFR rabbit IgG (Santa Cruz) and anti-IGF-1R mouse IgG (Santa Cruz) for 3 h at RT. The secondary antibodies conjugated with oligonucleotide plus or minus probes were diluted with 10% bovine serum in PBS and were added to the cells after they were washed twice in Tris-buffered saline containing Tween 20. The cells were incubated for 1 h at 37°C. After probe hybridization, they were washed twice with wash buffer A supplied in the Duolink kit and then incubated in a solution containing ligase for 30 min at 37°C. After washing, polymerase was added to the amplification solution and the mixture was incubated for 1 h 40 min at 37°C. Cells were washed twice in wash buffer B from the kit and the nuclei were counterstained with DAPI. Images were obtained using a Delta Vision fluorescence microscope (Applied Precision) and analyzed using the Duolink®ImageTool (Olink Biosciences).

### Statistical analysis

*In vitro* results were expressed as the mean ± standard deviation (SD). All results were analyzed by Prism version 5 (GraphPad software) using the Student's *t*-test. *P < 0.05 was considered statically significant.

## ACKNOWLEDGEMENTS

We are grateful to Dr. Yosef Yarden (Weizmann Institute of Science, Israel) for his gift of the full-length EGFR plasmid. This study was supported by the Intramural Research Program of the Korea Institute of Science and Technology (KIST) and a Korea University Grant. This work was also supported by a National Research Foundation of Korea (NRF 2011-0028168) grant funded by the Korean government.

## REFERENCES

1. Rakha EA and Chan S (2011) Metastatic triple-negative breast cancer. Clin Oncol 23, 587-600
2. Nielsen TO, Hsu FD, Jensen K et al (2004) Immunohistochemical and clinical characterization of the basal-like subtype of invasive breast carcinoma. Clin Cancer Res 10,

5367-5374
3. McClelland RA, Barrow D, Madden TA et al (2001) Enhanced epidermal growth factor receptor signaling in MCF7 breast cancer cells after long-term culture in the presence of the pure antiestrogen ICI 182,780 (Faslodex). Endocrinology 142, 2776-2788
4. Knowlden JM, Hutcheson IR, Jones HE et al (2003) Elevated levels of epidermal growth factor receptor/c-erbB2 heterodimers mediate an autocrine growth regulatory pathway in tamoxifen-resistant MCF-7 cells. Endocrinology 144, 1032-1044
5. Jin Q and Esteva FJ (2008) Cross-talk between the ErbB/HER family and the type I insulin-like growth factor receptor signaling pathway in breast cancer. J Mammary Gland Biol Neoplasia 13, 485-498
6. Jones HE, Goddard L, Gee JM et al (2004) Insulin-like growth factor-I receptor signalling and acquired resistance to gefitinib (ZD1839; Iressa) in human breast and prostate cancer cells. Endocr Relat Cancer 11, 793-814
7. Chakravarti A, Loeffler JS and Dyson NJ (2002) Insulin-like growth factor receptor I mediates resistance to anti-epidermal growth factor receptor therapy in primary human glioblastoma cells through continued activation of phosphoinositide 3-kinase signaling. Cancer Res 62, 200-207
8. Liu B, Fang M, Lu Y, Mendelsohn J and Fan Z (2001) Fibroblast growth factor and insulin-like growth factor differentially modulate the apoptosis and G1 arrest induced by anti-epidermal growth factor receptor monoclonal antibody. Oncogene 20, 1913-1922
9. Morgillo F, Woo JK, Kim ES, Hong WK and Lee HY (2006) Heterodimerization of insulin-like growth factor receptor/epidermal growth factor receptor and induction of survivin expression counteract the antitumor action of erlotinib. Cancer Res 66, 10100-10111
10. Sachdev D and Yee D (2006) Inhibitors of insulin-like growth factor signaling: a therapeutic approach for breast cancer. J Mammary Gland Biol Neoplasia 11, 27-39
11. Yarden Y and Sliwkowski MX (2001) Untangling the ErbB signalling network. Nat Rev Mol Cell Biol 2, 127-137
12. Lehmann BD, Bauer JA, Chen X et al (2011) Identification of human triple-negative breast cancer subtypes and preclinical models for selection of targeted therapies. J Clin Invest 121, 2750-2767
13. Yamasaki F, Zhang D, Bartholomeusz C et al (2007) Sensitivity of breast cancer cells to erlotinib depends on cyclin-dependent kinase 2 activity. Mol Cancer Ther 6, 2168-2177
14. DiGiovanni J, Kiguchi K, Frijhoff A et al (2000) Deregulated expression of insulin-like growth factor 1 in prostate epithelium leads to neoplasia in transgenic mice. Proc Natl Acad Sci U S A 97, 3455-3460
15. Carboni JM, Lee AV, Hadsell DL et al (2005) Tumor development by transgenic expression of a constitutively active insulin-like growth factor I receptor. Cancer Res 65, 3781-3787
16. Lee CT, Park KH, Adachi Y et al (2003) Recombinant adenoviruses expressing dominant negative insulin-like growth factor-I receptor demonstrate antitumor effects on lung cancer. Cancer Gene Ther 10, 57-63
17. Gallagher EJ and LeRoith D (2010) The proliferating role of insulin and insulin-like growth factors in cancer. Trends Endocrinol Metab 21, 610-618
18. Pollak M (2008) Targeting insulin and insulin-like growth factor signalling in oncology. Curr Opin Pharmacol 8, 384-392
19. Pollak M (2008) Insulin and insulin-like growth factor signalling in neoplasia. Nat Rev Cancer 8, 915-928
20. Fierz Y, Novosyadlyy R, Vijayakumar A, Yakar S and LeRoith D (2010) Insulin-sensitizing therapy attenuates type 2 diabetes-mediated mammary tumor progression. Diabetes 59, 686-693
21. Carboni JM, Wittman M, Yang Z et al (2009) BMS-754807, a small molecule inhibitor of insulin-like growth factor-1R/IR. Mol Cancer Ther 8, 3341-3349
22. Haluska P, Carboni JM, TenEyck C et al (2008) HER receptor signaling confers resistance to the insulin-like growth factor-I receptor inhibitor, BMS-536924. Mol Cancer Ther 7, 2589-2598
23. Fan QW, Cheng CK, Nicolaides TP et al (2007) A dual phosphoinositide-3-kinase alpha/mTOR inhibitor cooperates with blockade of epidermal growth factor receptor in PTEN-mutant glioma. Cancer Res 67, 7960-7965
24. Jones RB, Gordus A, Krall JA and MacBeath G (2006) A quantitative protein interaction network for the ErbB receptors using protein microarrays. Nature 439, 168-174
25. Riedemann J, Takiguchi M, Sohail M and Macaulay VM (2007) The EGF receptor interacts with the type 1 IGF receptor and regulates its stability. Biochem Biophys Res Commun 355, 707-714
26. Ryu JH, Shin M, Kim SA et al (2013) In vivo fluorescence imaging for cancer diagnosis using receptor-targeted epidermal growth factor-based nanoprobe. Biomaterials 34, 9149-9159